The importance of water to oceanic mantle melting regimes

P. D. Asimow* & C. H. Langmuir†

* *Division of Geological and Planetary Sciences, California Institute of Technology, Pasadena, California 91125, USA*
† *Department of Earth and Planetary Sciences, Harvard University, Cambridge, Massachusetts 02138, USA*

The formation of basaltic crust at mid-ocean ridges and ocean islands provides a window into the compositional and thermal state of the Earth's upper mantle. But the interpretation of geochemical and crustal-thickness data in terms of magma source parameters depends on our understanding of the melting, melt-extraction and differentiation processes that intervene between the magma source and the crust. Much of the quantitative theory developed to model these processes has neglected the role of water in the mantle and in magma, despite the observed presence of water in ocean-floor basalts. Here we extend two quantitative models of ridge melting, mixing and fractionation to show that the addition of water can cause an increase in total melt production and crustal thickness while causing a decrease in mean extent of melting. This may help to resolve several enigmatic observations in the major- and trace-element chemistry of both normal and hotspot-affected ridge basalts.

Much of the correlated variability among lava chemistry, crustal thickness, and axial depth observed along the global mid-ocean ridge system can be explained with reference to polybaric, anhydrous melting of peridotite[1–4]. The principal variable in this melting process is mantle potential temperature[3,4], modified by effects such as conduction to the surface[5–8], geometry of mantle flow (passive versus buoyancy-driven circulation)[7,9], extent of equilibration between migrating melts and mantle[2,7,10], and possibly major-element source composition. However, certain geochemically and bathymetrically anomalous regions such as the Galápagos[7] and Azores[11] platforms do not fit the global trends of variability, and are characterized by high concentrations of dissolved H_2O in erupted basalt glass[12]. Here we demonstrate with two models how the significant effects of H_2O on melting[13] and differentiation[14] affect the mean properties that are calculated for the ocean-ridge melting regime. In contrast to anhydrous melting processes, H_2O in the source increases the total melt production (and hence crustal thickness) and mean pressure of melting while decreasing the mean extent of melting. This model accounts for many features of the anomalous regions, and also is able to resolve a conflict between variations in major and trace elements on normal ocean ridges.

Two useful properties that summarize mantle melt production beneath ocean ridges are the mean (or bulk) extent of melting, F_B (ref. 15), and the crustal thickness, Z_c. F_B is defined as the mass of melt generated per unit time over the whole melting regime divided by the mass flux of subsolidus source into the melting regime. It follows that the enrichment of a perfectly incompatible tracer in the aggregate primary melt over its source is $1/F_B$. Furthermore, for most steady-state melting regimes there is a residual mantle column[16] (RMC) such that the crustal thickness in pressure units (which can be converted to kilometres from an estimate of crustal density) is given by F_B times the difference in pressure between the final pressure of melting (P_f) and the maximum pressure of residual material from which melt is extracted—which in many cases is the initial pressure of melting (P_o) (ref. 16). The 'shape' of the melting regime and the presence of active flow do not change the relation between F_B and Z_c (ref. 16), and only in cases where the depth to the solidus varies across axis, or melt is retained in some deep off-axis interval, is the connection to P_o obscured. For a model with near-constant productivity (that is, percentage melting per unit pressure drop), F_B increases linearly and Z_c quadratically with P_o, which in turn increases monotonically with potential temperature (T_P). Therefore F_B, mean pressure of melting ($\bar{P}$) and Z_c all correlate positively[3]. Furthermore, most complications to this scheme, such as modifications to the productivity function, the extent of buoyancy-driven active flow, or the physical mechanisms of melt extraction, still yield a direct proportionality among these parameters. These relationships among P_o, $\bar{P}$, F_B and Z_c also satisfy common sense—higher temperatures lead to a larger melting interval, more melt and thicker ocean crust. This model also accounts well for the major-element and bathymetric data from normal ridges not influenced by hotspots[7].

A partial exception to the correlation of all these parameters can occur with varying thicknesses of the lithospheric cap to the melting regime. For constant P_o, increasing lid thickness causes an increase in $\bar{P}$ but a decrease in extent of melting and crustal thickness, an effect that has been shown to be important for spreading rates less than 2 cm yr^{-1} (refs 6, 8). In this case as well, however, F_B and Z_c still correlate positively as the lid thickens.

These relationships do not take into account, however, the effect of water on mantle melting (Fig. 1). Water lowers the melting temperature of the mantle, and the addition of water to the source at constant potential temperature (T_P) causes melting to begin at a much higher pressure[6,17]. But because water is strongly concentrated in the liquid and the amount of water is small, it is diluted by further melting higher in the melting column and has little effect on the maximum extent of melting[18,19]. The net effect is to expand greatly the melting column by creating a large pressure interval at the base of the melting regime with very small amounts of melt present. The effects of this on F_B can be readily understood by considering that in a passive-flow, triangular melting regime, deepening the solidus by adding water increases the area of mantle flow that crosses the solidus, thereby increasing the denominator in the definition of F_B (ref. 15). The numerator is increased minimally because the productivity of deep hydrous melting is very small, hence the value of F_B decreases. Qualitatively, then, addition of water can reduce the mean extent of melting while leading to a small increase in crustal thickness.

Quantitative hydrous ridge models

We quantitatively demonstrate this effect with two models we have developed that add the effects of water to existing models of polybaric mid-ocean-ridge basalt melting and mixing. The model of ref. 7 (here called LKP), which is primarily based on olivine–liquid equilibria, has been modified by incorporating H cations as a simple diluent of other liquid species in the expression for the

olivine–liquid partition coefficient for Mg. This lowers the temperature of olivine–liquid equilibria linearly with liquid water content, and reproduces the experimental data of ref. 13. Here we call this model hLKP; for a more detailed reparameterization of wet melting with a similar approach, see ref. 20. The second model, pHMELTS, combines the thermodynamic melting model pMELTS[21] with estimates of water solubility in nominally anhydrous minerals from the compilation in ref. 18; a detailed assessment of this model will be presented elsewhere (P.D.A., J. E. Dixon and C.H.L., manuscript in preparation). The effects of variations in potential temperature, water content, and other variables on the relationship between F_B and Z_c for both models are shown in Fig. 2. The model predictions differ in many details but the essential results are very similar. Most notably, for dry, passive-flow melting regimes with melting continuing to the base of the crust, increases in potential temperature increase both F_B and Z_c along concave-down curves, as expected. In both models the addition of water at constant potential temperature generates a steeply decreasing negative trend, such that F_B drops by a factor of two and crustal thickness increases by ~1 km between 0 and ~700 p.p.m. H_2O in the source (Fig. 2). Changing other parameters of melting does not alter the essential results: a variation from passive to active flow (keeping the depth to the solidus and the depth of the RMC equal) or an increase in the final pressure of melting both lead to positive correlation between F_B and Z_c. Addition of water, however, with other variables held constant, leads to a decrease in F_B for all these schemes, no matter whether melting is fractional, continuous or equilibrium.

The effect of water is counter-intuitive because it permits greater melt production at lower mean extents of melting. Because the concentrations of highly incompatible elements in the aggregate liquid are inversely proportional to the mean extent of melting, increasing enrichments of incompatible elements relative to the source can be associated with increased melt production and crustal thickness.

Hotspot-affected ridges

These effects of water are able to account for a number of previously enigmatic aspects of oceanic basalt petrogenesis. One of the curious features of 'hotspot' magmatism is that hot regions should generate more melt and thus cause dilution of incompatible elements, and yet they invariably have exceptionally high concentrations of these elements. Looking at trace-element chemistry alone, one would be driven to infer very low extents of melting[22], whereas increased crustal thickness and highly depleted residual peridotites imply higher extents of melting[23]. Although isotopic evidence shows that the sources must be enriched, it is nonetheless hard to establish the quantitative magnitude of the enrichment. As hotspots are also high in water, we suggest that the bulk extents of melting are lower than would be inferred from the thick crust and shallow bathymetry, and hence the incompatible trace-element enrichments in the mantle sources are significantly lower than would have been inferred otherwise.

A simple illustration of this point is shown in Fig. 3a, where enrichment relative to the source is shown for Ba/Sm and Sm/Yb ratios for melting models that generate constant crustal thickness with varying water contents. As the water content of the source increases, the mean extent of melting decreases, and incompatible trace-element enrichments (for example, Ba/Sm) increase substantially, even if the source composition remains unchanged. Likewise, water addition raises the pressure of onset of melting and hence significantly increases the fraction of melt generated in the presence of residual garnet, even at constant crustal thickness, resulting in a

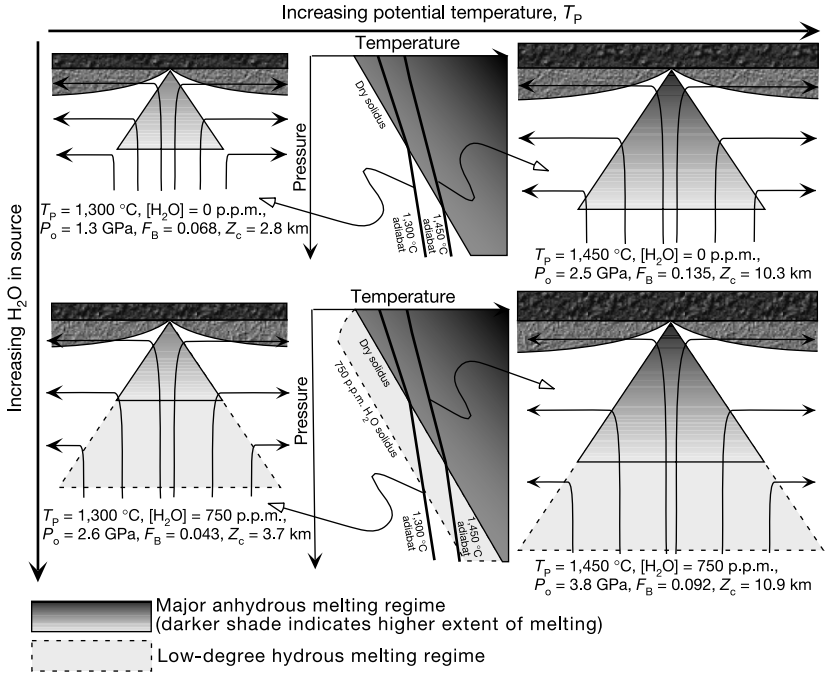

Figure 1 Conceptual models for the effects of potential temperature, T_P, and source H_2O concentration on mid-ocean-ridge melting regimes. Streamlines show a schematic passive corner flow in the asthenosphere. The shaded triangles indicate where melting is occurring. Variations in T_P control the depth at which adiabatically ascending mantle of a given composition crosses its solidus and begins melting. The presence of water induces an interval of low-productivity, low-degree melting below the level at which dry melting would begin. Increasing the water concentration increases the width of this interval, but high-productivity melting does not begin until near the pressure and temperature of the dry solidus. The maximum extent of melting reached increases with the pressure interval between the nominal dry solidus and the base of the lithosphere, and is sensitive to T_P but not to water addition. The mean extent of melting, F_B, is given by the pressure at the base of the extracted crust divided by the pressure interval of melting[15], and given the slopes of the wet and dry solidus curves and these productivity relations, F_B increases when extra crust is generated by an increase in T_P, but decreases when extra melting is driven by water addition. P_0, initial pressure of melting; Z_c, crustal thickness.

large increase in Sm/Yb. These coupled trace-element effects will be important in both ocean-ridge and ocean-island settings.

To explore the implications of these results in more detail, we examine data from two ocean ridges where depth and chemistry have been influenced by off-axis hotspots and are anomalous in a global context: the Galápagos spreading centre and the northern Mid-Atlantic Ridge near the Azores (Table 1). In both regions, high water contents are associated with shallow bathymetry[23–25] and enrichment in incompatible elements and radiogenic isotope ratios[23–25]. In the Galápagos, approaching longitude 91° W from either side, axial depth decreases from 2,800 m to ~1,700 m below sea level, the crustal thickness increases by ~2.5 km (refs 26, 27), and the fractionation-corrected water content of basalts reaches a peak with maximum values ~0.6 wt% (sources collected in the RIDGE petrological database[28]). These effects have previously been attributed[26], in the context of an anhydrous model, to a 50 °C increase in potential temperature; the anhydrous LKP or pMELTS models lead to similar results (Table 2). The Azores anomaly is similar but larger in magnitude: axial depth decreases from 3,500 to 1,200 m, crustal thickness increases by 3–4 km (ref. 29), and the fractionation and degassing-corrected water contents reach at least 0.9 wt% (ref. 12). Anhydrous melt production models

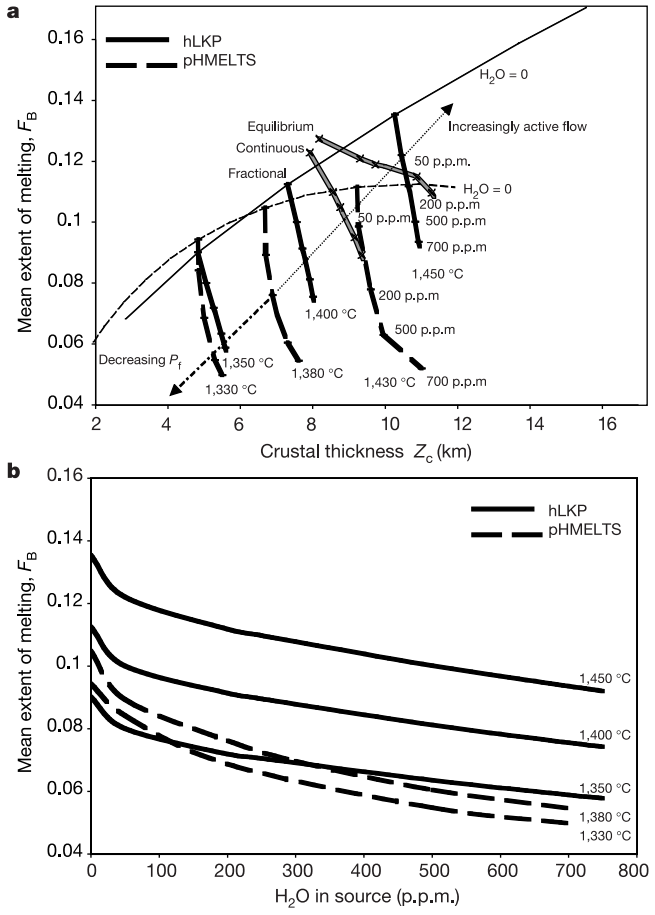

Figure 2 The relationships between mean extent of melting, F_B, crustal thickness, Z_c, and source H_2O content for mid-ocean-ridge melting regimes according to two models. The hLKP (continuous curves) and pHMELTS (dashed curves) models described in the text account for addition of water to the mantle source of mid-ocean-ridge basalts. **a**, F_B versus Z_c. The fine curves labelled '$H_2O = 0$' represent varying mantle T_P for dry sources in fractional fusion, passive-flow melting regimes[2,7]. The bold curves with tick marks at 50, 200, 500 and 700 p.p.m. H_2O by weight show the effects of water addition to fractional, passive melting regimes at constant T_P. The effects of water addition are similar for continuous (1% residual porosity) and equilibrium melting (shown by grey curves). Changes to the parameters of the melting regimes such as increasing the pressure of final melting, P_f, due to conductive cooling (dot-dashed arrow towards origin) or a transition from passive flow towards pure active flow[9] (dotted arrow away from origin) generate directly proportional changes in F_B and Z_c. **b**, The effect of source H_2O addition on F_B at constant T_P according to the hLKP (continuous curves) and pHMELTS (dashed curves) models.

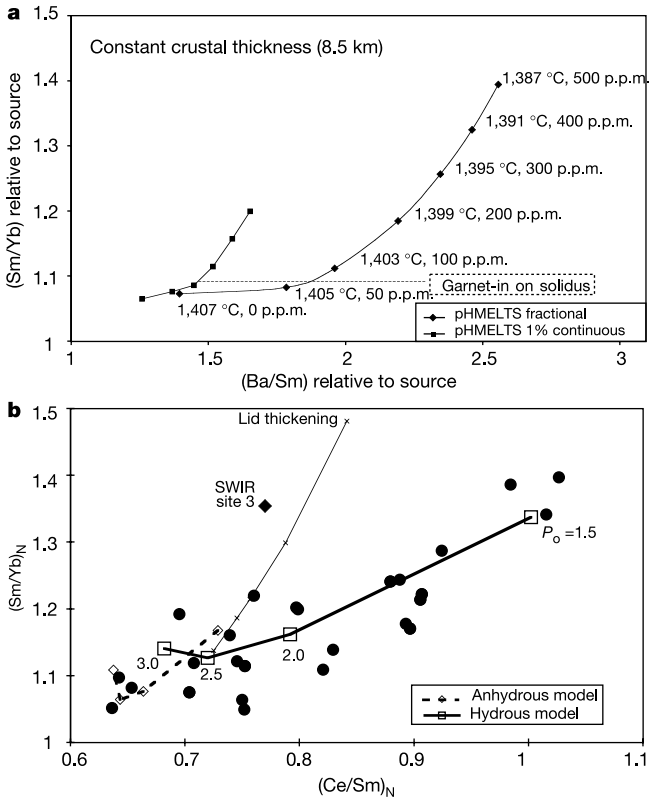

Figure 3 Trace-element systematics are strongly sensitive to the effects of water in the melting regime on both normal and hotspot-affected ridges. **a**, The presence of water changes the source region trace-element ratios that would be inferred from measured ratios in basalts and observations of Z_c. Results are shown for the pHMELTS model with perfect fractional melting or continuous melting with 1% residual porosity. These calculations all yield 8.5 km of crust from a passive-flow melting regime; Z_c is held constant by lowering T_P as water content increases; points are labelled by T_P and source H_2O content. The drop in mean extent of melting associated with increasing water content causes an increase in (Ba/Sm) relative to the source. The increasing influence of garnet as water deepens the solidus is reflected in the increase in (Sm/Yb) relative to the source. **b**, Models of the rare-earth element ratios of isotopically normal MORB. Data points are segment-averaged, primitive-mantle-normalized $(Sm/Yb)_N$ versus $(Ce/Sm)_N$ for global ridge segments chosen with average $^{87}Sr/^{86}Sr$ between 0.7025 and 0.70265 to remove the effects of mantle heterogeneity, from the compilation in ref. 32. The global trend caused by mantle temperature variations in an anhydrous model with a homogenous source produces a very small range in this diagram. Addition of a constant 150 p.p.m. H_2O to the source, on the other hand, lowers F_B while increasing the ratio of maximum to minimum F_B, which gives the necessary range in $(Ce/Sm)_N$ while increasing the contribution of melt from the garnet peridotite stability field and thereby raising $(Sm/Yb)_N$ at the cold end. The point 'site 3' is from ref. 6, and lies above the global trend at a position best explained by imposition of a conductively cooled lid. Calculations for fractional melting are carried out by recalculating mineral assemblages every 1 kbar of pressure ascent using equations in ref. 7. Boxes on the 'hydrous model' curve are labelled by pressure of initial solidus intersection, P_o, in GPa. For anhydrous calculations, source concentrations of Ce, Sm and Yb are respectively 0.77, 0.32 and 0.45 p.p.m; for hydrous calculations, 0.70, 0.31 and 0.44 p.p.m. are used. Partition coefficients for Ce, Sm and Yb are 0.086, 0.29 and 0.45 (clinopyroxene); 0.005, 0.02 and 0.11 (orthopyroxene); 0.008, 0.22 and 5 (garnet).

Table 1 **Segment-average properties away from and near hotspot influence**

	Long./lat.	Axial depth (m)	Crustal thickness (km)	Fe_8	$(H_2O)_8$	$(La/Sm)_N$
Galápagos	85–87° W	2,560	6	10.7	0.2	0.63
	90–92° W	1,650	8.5	9.6	0.45	1.37
Azores	33–35° N	2,870	6	10.0	0.18	0.76
	38–39.5° N	1,565	10	7.8	0.73	2.46

See text for details. Data are from refs 11, 12, 26, 28 and 29. Fe_8, total Fe as FeO corrected to 8 wt% MgO; $(H_2O)_8$, total dissolved H_2O corrected for degassing and fractionation to 8 wt% MgO; $(La/Sm)_N$, primitive-mantle-normalized ratio.

(Table 2) require a 75 °C temperature anomaly to generate the crustal thickness increase at the Azores platform. Concentrations and enrichment ratios of incompatible elements increase substantially as the depth shoals in both regions. The higher potential temperatures cause anhydrous models to predict increases of 10–30% in F_B at both the Galápagos and the Azores such that implied incompatible trace-element enrichments in the sources are significantly larger than the observed increases in the lavas. For example, treating water as a passive incompatible tracer, the implied water contents of the sources would reach ~400 p.p.m. for the Galápagos spreading centre and 650–800 p.p.m. for the Azores platform.

When instead we use hydrous melting models that produce the observed amount of water in the basalts and crustal thickness changes, we find that the Galápagos anomaly is explained by ≤300 p.p.m. H_2O in the source and an increase of ~40 °C in potential temperature, whereas the Azores anomaly is consistent with a peak of 500–600 p.p.m. H_2O in the source and a potential temperature anomaly of ~55 °C. In each case F_B drops by 40–60% approaching the most enriched regions, such that the source concentrations of incompatible elements need only increase by half as much as the observed increase in the enriched lavas (Table 2).

The importance of water to melting in these regions can be tested by investigating the effects on major-element compositions of basalts, which in these regions have substantially lower FeO at given MgO than basalts from equivalent depths elsewhere in the oceans. These low FeO values are not accounted for by the anhydrous mantle temperature model, as increasing potential temperature normally leads to deep melting and high FeO at given MgO (ref. 3) (Fig. 4). The effects of water on FeO can be evaluated by using the calculations above that constrain mantle temperature and extent of melting to calculate major-element compositions of mantle melts and then simulating fractionation of the melts for comparison to measured samples at equal MgO.

The calculations include the influence of water on the primary melt composition, but the dominant effect of water is the suppression of plagioclase crystallization. This leads to low FeO* (total Fe expressed as FeO) in samples fractionated to 8% MgO (Fig. 4b)[14], as expressed by the calculated parameter Fe_8. In the anhydrous calculations, the increases in potential temperature sufficient to generate the increased crustal thickness at the Galápagos or the Azores would lead to increases of 1–2% absolute in Fe_8—inconsistent with the data. On the other hand, using the hydrous hLKP or pHMELTS models, the increases in source water and smaller increases in potential temperature needed to match both crustal thickness and observed water contents lead to decreases of 1–2% absolute in Fe_8, consistent with the observations (Fig. 4a). Other major-element features of the data are also accounted for: the shallowest, most water-rich samples at both locations have high Al_8 and Ca_8 (ref. 11). Na_8 increases somewhat in the Galápagos, but is nearly constant over the Azores platform. High Al_8 and Ca_8 in multiply saturated samples are also signatures of enhanced crystallization of olivine (relative to plagioclase and clinopyroxene) owing to water. At the Azores, the combined effects of decreasing F_B and decreasing extent of fractionation to reach 8% MgO yield nearly constant Na_8 with no need for additional Na_2O in the source, whereas a dry model would require a significant Na_2O enrichment in the source to compensate for increasing extents of melting.

Si_8 is also low for the most water-rich samples. This reflects an increase in the mean pressure of melting, which is consistent with deep water-enhanced melting and/or an increase in potential temperature. Increased pressure is also indicated by a much stronger garnet influence on the trace-element patterns of the most water-rich lavas[25]. Therefore addition of water clearly can lead to increased garnet influence and greater pressures of melting—at the same time as mean extents of melting are reduced (Fig. 3a).

The result that water addition causes a decrease in the mean extent of melting appears contrary to the results of ref. 30—a linear increase in extent of melting with addition of H_2O to the source of a suite of Mariana back-arc lavas. That study, however, examined

Table 2 **Model results**

	Long./lat.	Model	T_P, source H_2O	F_B	Fe_8	Inferred source $(La/Sm)_N$
Galápagos	85–87° W	LKP dry	1,375 °C, 0	0.101	10.7	0.54
		hLKP wet	1,369 °C, 110 p.p.m.	0.082	10.6	0.49
		pMELTS dry	1,353 °C, 0	0.097	10.0	0.49
		pHMELTS wet	1,350 °C, 85 p.p.m.	0.065	10.5	0.44
Galápagos	90–92° W	LKP dry	1421 °C, 0	0.122	11.7	1.23
		hLKP wet	1,412 °C, 375 p.p.m.	0.090	9.1	1.09
		pMELTS dry	1,407 °C, 0	0.107	11.5	1.09
		pHMELTS wet	1,395 °C, 300 p.p.m.	0.055	10.5	0.80
Azores	33–35° N	LKP dry	1,375 °C, 0	0.101	10.7	0.65
		hLKP wet	1,369 °C, 100 p.p.m.	0.082	10.6	0.59
		pMELTS dry	1,353 °C, 0	0.097	10.0	0.59
		pHMELTS wet	1,350 °C, 75 p.p.m.	0.065	10.5	0.53
Azores	38–39.5° N	LKP dry	1,447 °C, 0	0.134	11.9	2.24
		hLKP wet	1,436 °C, 625 p.p.m.	0.091	9.1	1.95
		pMELTS dry	1,432 °C, 0	0.109	12.3	1.95
		pHMELTS wet	1,405 °C, 500 p.p.m.	0.054	9.5	1.31

See text for details of models. T_P, potential temperature; F_B, mean extent of melting.

individual samples from a single ridge segment, and the consistency of that result with isothermal addition of H_2O to peridotite[21] implies a small length scale of heterogeneity. Small water-rich heterogeneities are buffered to the temperature of surrounding peridotite, and therefore simply melt more at the same pressure as the adjoining anhydrous regions. Our results apply to pooled melts from the entire melting regime, where regional enrichments in source water content produce a large low extent of melting (F) tail deep in the melting regime. So although increased water in back-arc spreading centres may have a diagnostic chemical signature, it need not necessarily lead to larger mean extents of melting for the entire melting regime. For convergent margins, however, where there is no passive melting regime, increased water probably leads to both greater melt production and increased extents of melting. Understanding the effects of water in different tectonic settings requires combined examination of mantle flow patterns and the distribution and influence of water on melting.

Global consequences

The importance of the low-F tail produced by water is not limited to regions of enhanced water content such as the Azores and Galápagos. Even at the lower water contents of normal ocean ridges, water will create a substantial low-F tail that extends deeper into the mantle. This will lower the mean F relative to anhydrous calculations. The effect is greater for colder mantle, because an equivalent low-F tail then is larger relative to the smaller, cold melting regime. This means that the ratio of minimum to maximum F_B for the global ocean-ridge system is greater when water is taken into account. The tail also allows a role for residual garnet in regions too cold for the anhydrous solidus to encounter garnet peridotite[6,31]. Examination of global data for the rare-earth elements (REE) shows that both these effects are required for REE models to be consistent with major-element models for a homogeneous mantle source. Figure 3b shows REE data for normal ocean ridges from the RIDGE petrology database[28], screened to remove as much as possible the effects of mantle heterogeneity by choosing only ridge segments with mean $^{87}Sr/^{86}Sr$ from 0.7025 to 0.70265. There is no correlation within this subset between isotopes and trace-element enrichments. Although isotopic enrichment is associated with hotspots and thickened crust, in this isotopically filtered subset the highest light-REE enrichments are instead systematically from regions of thin crust. The anhydrous melting calculations are unable to produce the substantial range in either primitive-mantle-normalized $(Ce/Sm)_N$ or $(Sm/Yb)_N$ through variations in potential

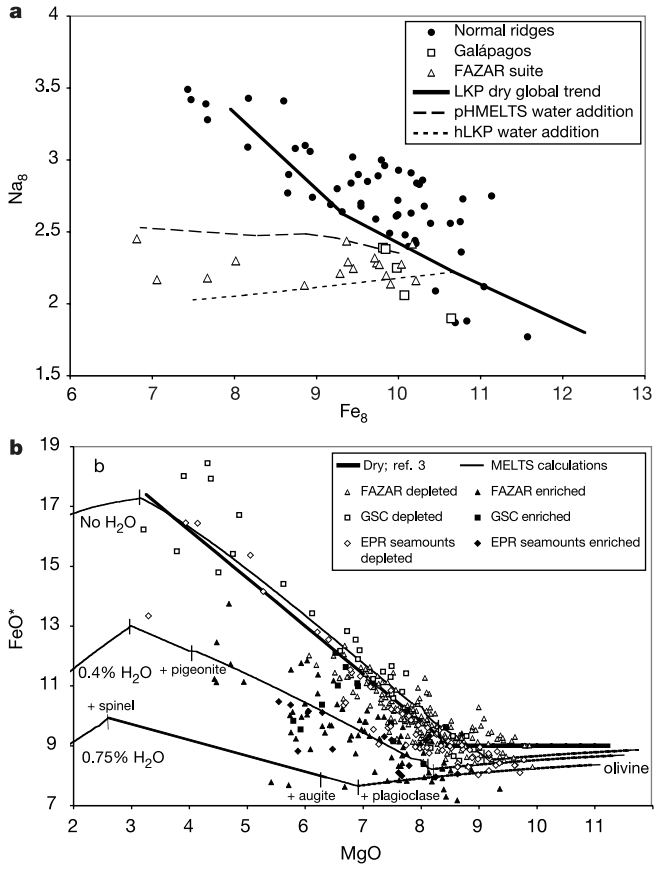

Figure 4 The influence of water on fractionation-corrected major-element composition of MORB. **a**, Segment-scale averages of FeO* (total Fe expressed as FeO) and Na_2O concentrations in ocean-ridge basalts corrected for fractionation to 8% MgO, giving Fe_8 and Na_8, respectively. The correction used the standard liquid line of descent given in ref. 3, which assumes that all mid-ocean-ridge basalts fractionate along a parallel trend in oxide versus MgO space with multiple saturation beginning at 8.5% MgO. The normal (that is, non-hotspot affected) ridge segments are well described by the global trend of T_P variations according to the dry LKP model[7], but the Galápagos- and especially the Azores-affected segments have Fe_8 much too low for their Na_8 and Z_c values. However, addition of up to 750 p.p.m. water at constant T_P in either the hLKP or pHMELTS models causes apparent Fe_8 to decrease by ≥3 wt% at nearly constant Na_8 (accompanied by a ~1 km increase in Z_c, see Fig. 2). **b**, The decrease in Fe_8 is dominated not by melting effects but by the effect of H_2O on low-pressure differentiation, where it both suppresses multiple saturation with plagioclase to lower MgO and decreases the slope of the multiply saturated liquid line of descent in FeO*–MgO space[14]. The low FeO at any given MgO is a real effect generated by delay of multiple saturation during forward fractionation of primitive samples, whereas the low Fe_8 of water-rich samples in **a** is partly an artefact of correcting data back to 8% MgO using a liquid line of descent slope only appropriate for dry normal basalts. GSC is the Galápagos Spreading Centre; FAZAR is the Mid-Atlantic suite near the Azores[11]. For this figure, the boundary between 'depleted' and 'enriched' is $K_2O/TiO_2 = 0.25$ for FAZAR, 0.11 for GSC, and 0.25 for East Pacific Rise (EPR) seamounts.

temperature[5]. On the other hand, varying mantle potential temperature with constant water content of ~150 p.p.m. accounts well for the global data—indeed it appears to be essential to produce the necessary ranges of, and correlation between, crustal thickness and $(Ce/Sm)_N$ (as well as Na_8). An important implication is that the mantle source of normal MORB is more depleted (~10% lower in $(Ce/Sm)_N$) than would be inferred from anhydrous batch melting calculations.

A trend similar to the data in Fig. 3b can also be obtained from models where variable source heterogeneity is imposed by a source component carrying both water and incompatible elements at nearly constant potential temperature (such as we invoke above for hotspot-affected regions). To explain the isotopically normal ridge segments, however, this heterogeneity would have to be very young, and this model also would not account for the significant differences in crustal thickness. Note also that the effects of lithospheric lid thickening caused by surface cooling can be distinguished from mantle temperature variations or addition of low-*F* melt component by relatively high $(Sm/Yb)_N$ ratios, as observed for some, but not all, segments along the slow-spreading southwest Indian ridge[6], and the Gakkel ridge.

Finally, the reasoning behind the large effect of the low-*F* tail on cold mantle melting regimes can also be applied to hotspots that rise beneath thick lithosphere. A short melting column caused by the truncation of the melting regime by the lithosphere will also be strongly influenced by a long, low-*F* tail of melt. This effect could cause actual extents of melting to be a factor of two lower than inferred from anhydrous models, and sources to be correspondingly less enriched. □

Received 20 November 2002; accepted 14 January 2003; doi:10.1038/nature01429.

1. Dick, H. J. B., Fisher, R. L. & Bryan, W. B. Mineralogic variability of the uppermost mantle along mid-ocean ridges. *Earth Planet. Sci. Lett.* **69,** 88–106 (1984).
2. Asimow, P. D., Hirschmann, M. M. & Stolper, E. M. Calculation of peridotite partial melting from thermodynamic models of minerals and melts. IV. Adiabatic decompression and the composition and mean properties of mid-ocean ridge basalts. *J. Petrol.* **42,** 963–998 (2001).
3. Klein, E. M. & Langmuir, C. H. Global correlations of ocean ridge basalt chemistry with axial depth and crustal thickness. *J. Geophys. Res.* **92,** 8089–8115 (1987).
4. McKenzie, D. P. & Bickle, M. J. The volume and composition of melt generated by extension of the lithosphere. *J. Petrol.* **29,** 625–679 (1988).
5. Shen, Y. & Forsyth, D. W. Geochemical constraints on initial and final depths of melting beneath mid-ocean ridges. *J. Geophys. Res.* **100,** 2211–2237 (1995).
6. Robinson, C. J., Bickle, M. J., Minshull, T. A., White, R. S. & Nichols, A. R. L. Low degree melting under the Southwest Indian Ridge: the roles of mantle temperature, conductive cooling and wet melting. *Earth Planet. Sci. Lett.* **188,** 383–398 (2001).
7. Langmuir, C. H., Klein, E. M. & Plank, T. in *Mantle Flow and Melt Generation at Mid-Ocean Ridges* (eds Phipps Morgan, J., Blackman, D. K. & Sinton, J. M.) 183–280 (American Geophysical Union, Washington DC, 1992).
8. White, R. S., Minshull, T. A., Bickle, M. J. & Robinson, C. J. Melt generation at very slow-spreading oceanic ridges: Constraints from geochemical and geophysical data. *J. Petrol.* **42,** 1171–1196 (2001).
9. Forsyth, D. W. in *Mantle Flow and Melt Generation at Mid-Ocean Ridges* (eds Phipps Morgan, J., Blackman, D. K. & Sinton, J. M.) 1–66 (American Geophysical Union, Washington DC, 1992).
10. Johnson, K. T. M., Dick, H. J. B. & Shimizu, N. Melting in the oceanic upper mantle: An ion microprobe study of diopsides in abyssal peridotites. *J. Geophys. Res.* **95,** 2661–2678 (1990).
11. Asimow, P. D. & Langmuir, C. H. Segment-scale and regional systematics from 33 °N to 41 °N on the Mid-Atlantic Ridge: Results from the FAZAR Cruise. *Eos* **79,** F938–F939 (1998).
12. Dixon, J. E., Leist, L., Langmuir, C. H. & Schilling, J.-G. Recycled dehydrated lithosphere observed in plume-influenced mid-ocean-ridge basalt. *Nature* **420,** 385–389 (2002).
13. Gaetani, G. A. & Grove, T. L. The influence of water on melting of mantle peridotite. *Contrib. Mineral. Petrol.* **131,** 323–346 (1998).
14. Michael, P. J. & Chase, R. L. The influence of primary magma composition H_2O and pressure on mid-ocean ridge basalt differentiation. *Contrib. Mineral. Petrol.* **96,** 245–263 (1987).
15. Plank, T., Spiegelman, M., Langmuir, C. H. & Forsyth, D. W. The meaning of "mean F": Clarifying the mean extent of melting at ocean ridges. *J. Geophys. Res.* **100,** 15045–15052 (1995).
16. Plank, T. & Langmuir, C. H. Effects of the melting regime on the composition of oceanic crust. *J. Geophys. Res.* **97,** 19749–19770 (1992).
17. McKenzie, D. The extraction of magma from the crust and mantle. *Earth Planet. Sci. Lett.* **74,** 81–91 (1985).
18. Hirth, G. & Kohlstedt, D. L. Water in the oceanic upper mantle: Implications for rheology, melt extraction and the evolution of the lithosphere. *Earth Planet. Sci. Lett.* **144,** 93–108 (1996).
19. Hirschmann, M. M., Asimow, P. D., Ghiorso, M. S. & Stolper, E. M. Calculation of peridotite partial melting from thermodynamic models of minerals and melts III. Controls on isobaric melt production and the effect of water on melt production. *J. Petrol.* **40,** 831–851 (1999).
20. Katz, R. F., Spiegelman, M. & Langmuir, C. H. Models of equilibrium and reactive melting in a subduction zone setting. *Geochem. Geophys. Geosyst.* (submitted).
21. Ghiorso, M. S., Hirschmann, M. M., Reiners, P. W. & Kress, V. C. The pMELTS: A revision of MELTS for improved calculation of phase relations and major element partitioning related to partial melting of the mantle to 3 GPa. *Geochem. Geophys. Geosyst.* **3,** 10.1029/2001GC000217 (2002).
22. Kay, R. W. & Gast, P. W. The rare earth content and origin of alkali-rich basalts. *J. Geol.* **81,** 653–682 (1973).
23. Bonatti, E. Not so hot "hot spots" in the oceanic mantle. *Science* **250,** 107–111 (1990).
24. Schilling, J.-G., Bergeron, M. B. & Evans, R. Halogens in the mantle beneath the North Atlantic. *Phil. Trans. R. Soc. Lond. A* **297,** 147–178 (1980).
25. Schilling, J.-G. Azores mantle blob: the rare earth evidence. *Earth Planet. Sci. Lett.* **25,** 103–115 (1975).
26. Ito, G. T. & Lin, J. Mantle temperature anomalies along the present and paleoaxes of the Galápagos spreading center as inferred from gravity analyses. *J. Geophys. Res.* **100,** 3733–3745 (1995).
27. Detrick, R. S. *et al.* Correlated geophysical, geochemical, and volcanological manifestations of plume-ridge interaction along the Galápagos Spreading Center. *Geochem. Geophys. Geosyst.* **3,** 10.1029/2002GC000350 (2002).
28. Lehnert, K., Su, Y., Langmuir, C. H., Sarbas, B. & Nohl, U. A global geochemical database structure for rocks. *Geochem. Geophys. Geosyst.* **1,** 10.1029/1999GC000026 (2000).
29. Detrick, R. S., Needham, H. D. & Renard, V. Gravity anomalies and crustal thickness variations along the Mid-Atlantic Ridge between 33°N and 40°N. *J. Geophys. Res.* **100,** 3767–3787 (1995).
30. Stolper, E. M. & Newman, S. The role of water in the petrogenesis of Mariana trough magmas. *Earth Planet. Sci. Lett.* **121,** 293–325 (1994).
31. Langmuir, C. H. Deep low *F* melts and the global systematics of MORB. *Eos* **76,** F694–F695 (1995).
32. Su, Y.-J. *Database Applications to the Petrogenesis of Ocean Ridge Basalts.* Thesis, Columbia Univ. (2002).

Acknowledgements We thank P. Michael for comments and suggestions. This work was supported by the National Science Foundation.

Competing interests statement The authors declare that they have no competing financial interests.

Correspondence and requests for materials should be addressed to P.D.A. (e-mail: asimow@gps.caltech.edu).